Soft Matter

Cite this: *Soft Matter*, 2011, **7**, 10039

www.rsc.org/softmatter

PAPER

Mechanics of carbon nanotube networks: microstructural evolution and optimal design†

Bo Xie, Yilun Liu, Yiting Ding, Quanshui Zheng and Zhiping Xu*

Received 3rd June 2011, Accepted 2nd August 2011
DOI: 10.1039/c1sm06034a

Carbon nanotube networks feature outstanding mechanical performance, and also hierarchical structures and network topologies. In this paper we investigate their structure–property relationship through mesoscale molecular dynamics simulations. We find that their microstructures undergo remarkable evolution under mechanical loads. The correlation between applied strain, microstructural evolution and failure mechanism, especially the bundling process and evolution of bridging carbon nanotubes, is discussed based on the simulation results. Based on the insights of the underlying mechanisms, further engineering approaches on the carbon nanotube networks towards enhanced mechanical properties are proposed and validated, *e.g.*, by including intertube cross-links that resist shear, maintain the network topology and improve strain affinity.

Introduction

Flexible and multifunctional material is one of the key technologies for future electronics and renewable energy.[1,2] Foldable and bendable materials, such as thin films and membranes made of composites or papers, for example, have caught significant interest recently. Exciting applications have appeared, including soft, portable rollup displays and wearable items. Low-dimensional carbon nanostructures are excellent candidates according to their outstanding mechanical and transport properties along the extensive directions, with simultaneously allowable bending and twisting deformations in other dimensions. Carbon nanotubes can sustain 20% elastic strain before fracture nucleates, and thus they are able to be bent reversibly with an extremely small radius of curvature of a few nanometres. This flexibility can even be further improved through localized buckling or rippling structures.[3,4] In addition to these amazing mechanical properties, the thermal, electrical and electrochemical properties of carbon nanostructures are also promising for multifunctional applications.

In the synthesis and processing of nanocomposites for large-scale applications, the dispersion of carbon nanostructures within the matrices and their interfaces are of critical importance to establish efficient load-bearing performance.[5] However, this problem has not been solved satisfactorily yet and awaits technical breakthroughs. On the other hand, networked materials such as buckypapers and graphene papers are intrinsically controlled by the carbon nanostructures as building blocks and network structures. The performance of the bulk material thus can be tuned more feasibly. A striking example is that the ultrathin buckypaper can be electrically conducting, 250 times stronger than steels while 10 times lighter. Moreover, a recent study shows temperature-invariant viscoelasticity from −196 °C to 1000 °C, in stark contrast to the silicone rubber that possesses a much narrower operating temperature range from −55 °C to 300 °C.[6]

Buckypapers usually feature a porous structure with a disordered arrangement of carbon nanotubes cross-linked by intertube interactions.[7–9] The mechanical properties of carbon nanotube networks and their transport mechanisms depend on the percolated load-bearing substructures. Thus the microstructure of carbon nanotube networks defines these properties and a rational design on this structure could lead to high-performance paper materials. To this end, in-depth insights on the relation between the microstructures and mechanical properties of carbon nanotubes are urged.

Like many other networked materials such as cytoskeleton networks and rubbers, both the properties of building blocks and their communications, *i.e.* cross-links, entanglements *etc.*, strongly affect their macroscopic properties.[10–15] In addition, these microstructures evolve under mechanical loads, which further modify mechanical properties, and also thermal and electrical performance. However, their correlation is still not well understood up to now. A synergetic study combining the power of molecular simulations and fine-scale microscopy observations is required. In this work, we perform coarse-grained (CG) molecular dynamics (MD) simulations to investigate the multi-scale mechanics of carbon nanotube networks, which are shown to be consistent with and complementary to available experimental evidences, which lays the groundwork for the rational

Department of Engineering Mechanics and Center for Nano and Micro Mechanics, Tsinghua University, Beijing, 100084, China. E-mail: xuzp@tsinghua.edu.cn

† Electronic supplementary information (ESI) available: Movies showing structural evolution of carbon nanotube networks under uniaxial (M1) and biaxial (M2) strain loading. See DOI: 10.1039/c1sm06034a

engineering design of nanostructured materials towards optimal mechanical performance.[14]

Materials and methods

Coarse-grained molecular dynamics

As full-atom molecular dynamics simulations cannot access the carbon nanotube networks with current computing resources, we use a coarse-grained model for carbon nanotubes, as described in ref. 14. In this model, discrete beads interacting through bond and bond angle springs provide a description equivalent to a continuum mechanics model with specific tension stiffness, and bending rigidity.

The mechanically relaxed network structure is illustrated in Fig. 1. Within each nanotube, the stretching energy contributions of two bonding beads are given by $E_T = k_T(r - r_0)^2/2$, where $k_T = YA/r_0$ is the spring constant relating to the tension stiffness, Y is the Young's modulus of the carbon nanotube, A is the cross-section area and r is the distance between two bonding beads with $r_0 = 1$ nm as its equilibrium distance. The bending energy contributions of adjacent beads triplets are given by $E_B = k_B(1 + \cos\varphi)$, where $k_B = 2YI/r_0$ is the angular spring constant relating to the bending stiffness $D = YI$ and φ is bending angle within the triplet. I is the bending moment of inertia. In addition, for intertube interactions, we define the van der Waals interactions between beads in different carbon nanotubes by a Lennard-Jones formula $E_{pair} = 4\varepsilon[(\sigma/r)^{12} - (\sigma/r)^6]$. The parameters can be found in ref. 14.

Samples preparation

The structure of our coarse-grained model is illustrated in Fig. 1. The structure of a carbon nanotube network is self-assembled from a random ensemble of individual nanotubes here instead of one with artificially defined microstructures such as bundles. A two-dimensional periodic boundary condition is used for in-plane directions x and y. The length and width of the periodic simulation box are 240 nm and 120 nm respectively. (5,5) carbon nanotubes with a length of 100 nm (100 beads) are firstly constructed with a uniform curvature, and deposited in a layer by layer manner subsequently.[14] The whole system consists of 10^4–10^5 beads in the layer thickness range we explore here. In principle the diameter and length of the carbon nanotubes can be extended to a larger scale, *e.g.* 10 nm and 10–100 μm respectively. However in this paper we will focus on the deformation and failure mechanisms, thus a representative system is chosen. The orientations of the nanotubes are uniformly distributed between 0 and π.

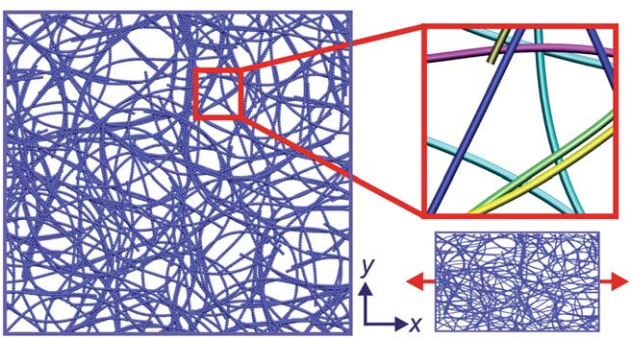

Fig. 1 A coarse-grained model for carbon nanotube networks. The uniaxial load is applied to the x direction of a super cell with two-dimensional in-plane periodic boundary conditions. The inset shows local structure of crossings. In the molecular dynamics simulation, intrafiber elasticity is described by a bond stretching and a bond angle bending term, reproducing the Young's modulus and bending rigidity of a carbon nanotube. The interfiber binding is captured by a Lennard-Jones type pair interaction between coarse-grained beads.

The microstructures of the carbon nanotubes network are equilibrated using a Langevin thermostat before mechanical loading. To accelerate the equilibrium process, a body force is initially applied and a rigid supporting substrate is added below to make the whole structure more compact, following the procedures in experiments.[6] After that, the force and substrate are both removed to maintain the membrane structure. The thermostat at 300 K is maintained for one microsecond until the fluctuation of total energy converges below 0.1%.

Mechanical loading

For uniaxial loading, tensile strain is applied in the x direction by deforming the simulation box as shown in Fig. 1. The loading rate v is 3 m s^{-1}. The equations of motion are integrated using a velocity-Verlet algorithm with a time step of 10 fs that ensures the numerical convergence of integration. The pressure in the transverse y direction is restrained as zero during the tensile loading process by using a Berendsen barostat. The tensile stress is calculated from the summation of virial stress over the buckypaper sample and the tensile force is calculated subsequently by multiplying the stress with the cross-section area. The deformation of the simulation box in both x and y directions is recorded for further strain analysis. For biaxial loading, the same strain rate is applied for both x and y directions. In the thickness direction z, no constraint is applied for both uniaxial and biaxial loading conditions.

Results

Equilibrated microstructures of carbon nanotube networks

A typical configuration of the carbon nanotube network after the equilibrating process is shown in Fig. 1. The network shows porous structures with pore size distributed up to six nanometres. Additionally, bundles where several nanotubes bind locally in parallel nucleate across the whole paper network, as driven by the surface tension due to intertube van der Waals interactions. For the relatively large supercell used for the network here in our simulations, distributions of intratube bond distances and angles show an isotropic equivalence in the x and y directions. The thickness h of a buckypaper in our simulations is defined as the maximum distance in the z direction of the sample. We prepare several samples with varying initial carbon nanotube densities n. The thickness of the equilibrated network firstly increases as a linear function of the density and then converges at 0.28 g cm^{-3}, corresponding to the equilibrium network density at ambient condition. This density level is close to the reported value for single-walled carbon nanotube based buckypapers.[16,17] In our

following discussion, we use simulation results starting from this structure.

Mechanical behavior under tension

As a tensile load is applied, the symmetry in the x direction and contraction in the y direction is broken due to the elongation, as shown in Fig. 1. A typical tensile force–strain curve is plotted in Fig. 2 for the sample with $h = 9.3$ nm. From the results we can see that this material features a tensile stiffness on the order of $K = 0.1$ N m^{-1}, corresponding to a Young's modulus of 21.5 MPa. This value obtained in our simulations is consistent and relatively slower than experimentally measured ones, which could arise from the existence of cross-links, entanglements and modified carbon nanotube surfaces that lead to stronger binding between carbon nanotubes in the network rather than bare van der Waals interactions here in our model.[16,17] These effects will be discussed in detail later in the text. By comparing simulation results for all the structures we prepare, we find that although the curves fluctuate due to the randomness of atomic positions, the characteristic behaviour and K values are universally on the same order for a specific network density.

To obtain some insights on the relation between microstructural characteristics and macroscopic mechanical behaviour, we decompose the tension force F sustained in the carbon nanotube networks into three terms attributed to bond stretching F_s, bond angle bending F_b and van der Waals interactions F_{pair} respectively, according to the energy functionals used in our MD simulations to determine the force acting on the atoms. As shown in Fig. 2, the total force firstly jumps up to 40 nN rapidly and then increases gradually before material failure at the strain ε of 1.0 as evidenced by a reduction of F. In the inset of Fig. 2, it can be clearly shown that this initial jump is attributed to increasing participation, or fastening, of intertube van der Waals interaction as will be discussed below, which then converges at a strain

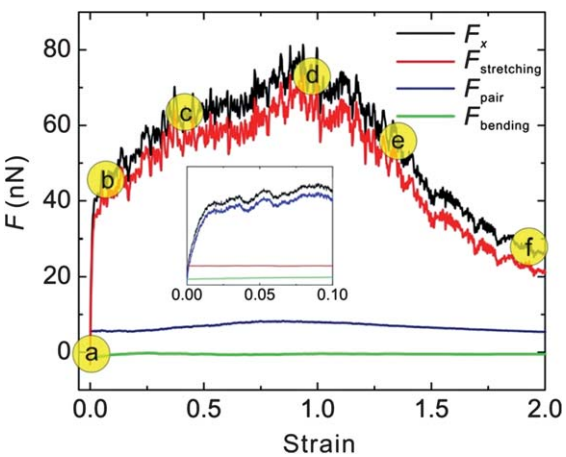

Fig. 2 The relation between a tensile force sustained in the carbon nanotube network and strain, with decompositions into contributions from bond stretching $F_{stretching}$ (tension), bond angle bending $F_{bending}$ (bending) and pair interactions F_{pair} (intertube binding). Force is used here instead of stress as the transverse direction of the supercell shrinks significantly as the tensile load is applied, leading to a drastic enhancement of the stress, while the tensile force is a more direct measurement for the load-bearing and transfer capabilities.

level of 0.0013. Afterwards, the bond stretching term F_s plays the dominant role, while the bond angle term F_b has less impact on the load-bearing in the x direction.

During the deformation under a uniaxial load, there is a remarkable contraction in the transverse direction, resulting from the rotation and sliding of carbon nanotubes. Before the onset of material failure starts, this transverse contraction ends at a constant value. To avoid the ambiguous definition for the rapidly changing cross-section area, we use the tensile force instead of the stress here to qualify the load-bearing and transfer capacities.

Mechanisms of microstructural evolution

In our simulations results, we find that the mechanical behaviour of carbon nanotubes under uniaxial tension is closely correlated to their microstructural evolution, which is shown in Fig. 3(a)–(f) and Movie M1 in the Electronic Supplementary Information.† In the beginning stage of uniaxial loading, local stretching of van der Waals binding sites leads to an affine deformation and the in-plane stress is uniform over the whole material (Fig. 3(a) and (b)). As the uniaxial tension increases, transverse contraction due to the Poisson's effect results in a compression of the porous network structures (Fig. 3(c)). In addition, there are distinct changes of the network topologies. Some carbon nanotubes bundle together and form several main threads across the material in the loading direction x that bear most of the load (Fig. 3(d) and (e)).

To quantitatively analyze the bundling process, we define an intertube distance by averaging the nearest neighbour distance over all bead pairs locating in adjacent carbon nanotubes. This measure is a summation of the radius of two carbon nanotubes and distance between their walls, which accounts for intertube separation, transplacement and rotation. The results of intertube distance distribution as summarized in Fig. 4 show that as tensile strain is applied, the average distance between carbon nanotubes decreases. A bundling process with an averaged intertube distance of 1 nm presents distinctly, which further converges as a final structure in Fig. 3(e) is formed. Moreover we identify from the simulation results that bundles with eight to eighteen carbon nanotubes are widely observed in this final structure.

As a result of this bundling process, the deformation field becomes non-affine and the network topology evolves remarkably. The network eventually breaks at some of these threads by losing intertube binding, but discrete blocks are as left isolated where local network structures are well preserved (Fig. 3(f)).

Based on these intuitive inspections on the dynamic evolution of network topologies, we further extract a few key structural evolution mechanisms that define the overall mechanical properties of the carbon nanotube networks.

In a distinct mechanism shown in Fig. 5(a), carbon nanotubes contact partially each other through van der Waals interactions and tend to increase the contact area through rotation and bending of carbon nanotubes, as driven by surface tension.[18] This mechanism eventually leads to rotation of carbon nanotubes and formation of thick carbon nanotube bundles with some twists.[7] The bending rigidity of these bundles, which is proportional to d^4 are much enhanced if compared with individual nanotubes of the same mass, where d is the fibre diameter. As the network with

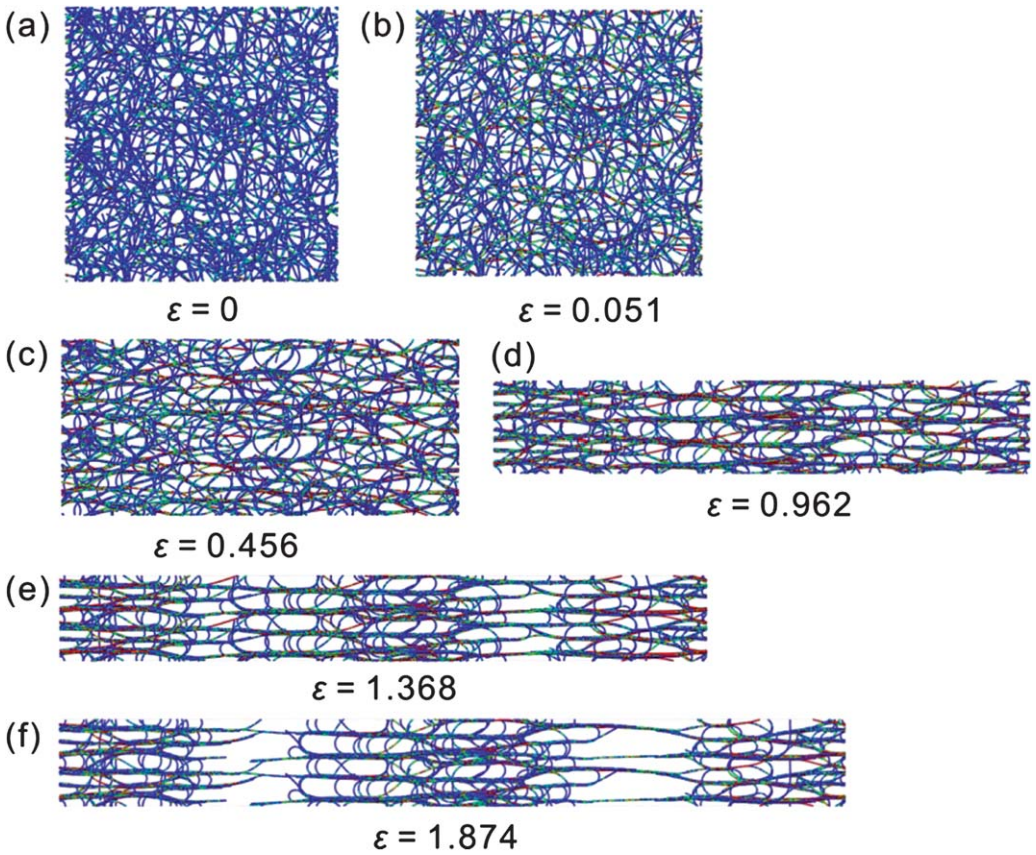

Fig. 3 Structural evolution of carbon nanotube networks under tensile loading, with a strain level at (a) 0%, (b) 0.051, (c) 0.456, (d) 0.962, (e) 1.368 and (f) 1.874 respectively. The colour maps stress amplitude along the tensile direction. The blue colour represents zero or compressive stress, while other colors indicate the tensile stress state and the red colour corresponds to maximum stress. The network structure is duplicated in the *y* direction for better illustration.

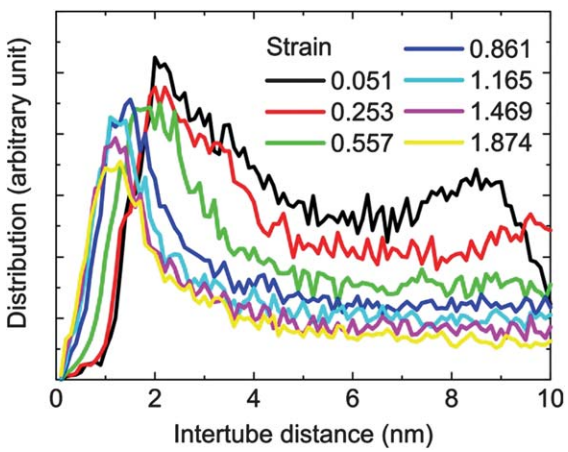

Fig. 4 Evolution of intertube distance distribution as uniaxial strain is applied, which shows distinctly the bundling process corresponding to an intertube distance of 1 nm.

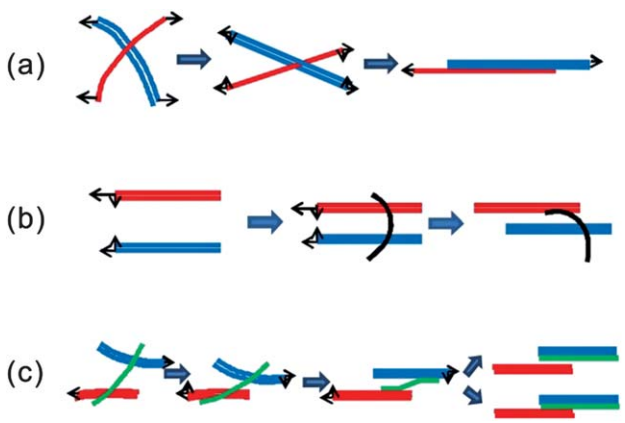

Fig. 5 (a)–(c) Typical mechanisms of microstructural evolution as a uniaxial tensile load is applied to the carbon nanotube networks.

locally bundled microstructures is further loaded in the *x* direction, intertube sliding will be initialized inside the bundles due to the low shear strength.[19] During this process, the potential energy from van der Waals interactions is firstly lowered due to the increasing of contact area, meanwhile the bending energy of carbon nanotubes decreases as in the bundled nanotubes are straightened (Fig. 6(c)). Then it increases slightly as the contact area within the bundle is reduced by shear deformation. The complexity of the network structure introduces a number of local minima on the potential energy landscape, which locks the local motion of nanotubes during network evolution. These locking events prohibit further formation of one single bundle consisting

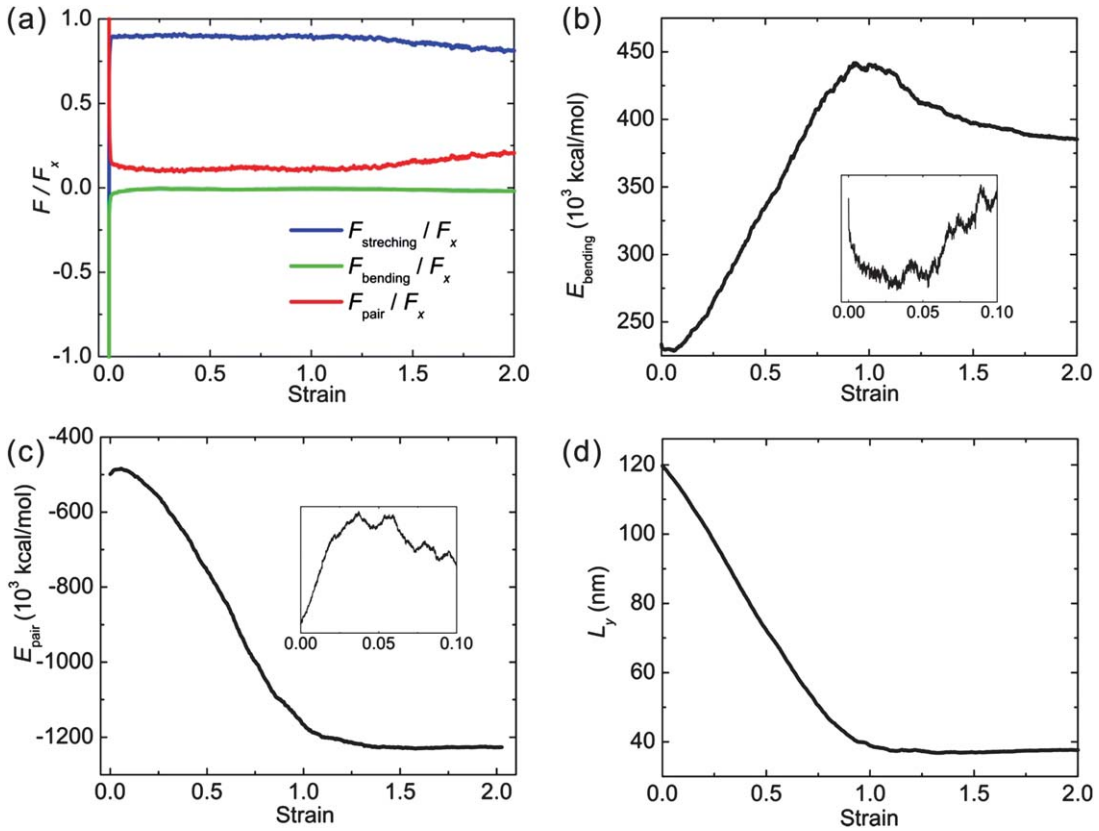

Fig. 6 (a)–(c) Force F, bending and pair energy evolution under uniaxial strain loading. (d) Transverse contraction (L_y) of carbon nanotube networks.

of all the nanotubes that apparently is the state locating at the global minimum of the potential energy landscape.

As discussed above, one of the most significant driving forces for the bundling process is strain-induced alignment of carbon nanotubes as indicated in Fig. 5(a). The orientation of carbon nanotubes, as defined by the angle they orient with the x-direction, is plotted in Fig. 7. It is shown that as strain increases, the orientation of carbon nanotubes becomes more concentrated and in parallel to the loading direction x, accompanied with significant transverse contraction in the y-direction (Fig. 6(d)).

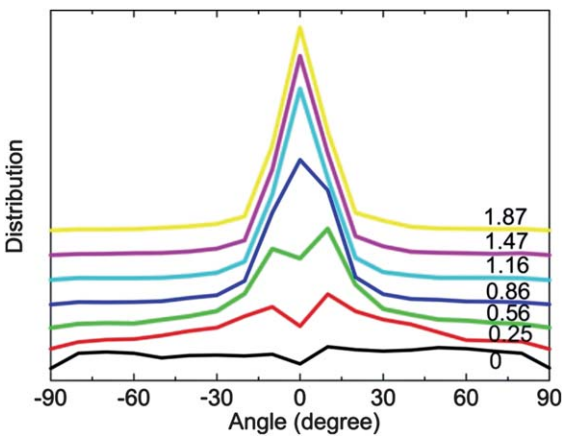

Fig. 7 Evolution of orientational angle distribution under uniaxial strain.

There exist many carbon nanotubes that bridge other nanotubes through van der Waals interactions. When the carbon nanotubes that are bridged move closer due to the transverse contraction, the bridging nanotube will be bent (Fig. 5(b)), which results in the increasing of bending energies, as shown in Fig. 6(b). When the energy associated with the bending deformation is too large to be maintained by the van der Waals interactions at end contacts, bent carbon nanotubes will detach to release bending energy.

On the other hand, when carbon nanotubes are bridging two distant carbon nanotubes that are moving in opposite directions, alignment of the bridging nanotube and increasing of the intertube contact will be induced as shown in Fig. 5(c). This process will firstly enhance the resistance of the whole network to uniaxial loads by increasing intertube load transfer. However, the bridge structure will eventually disappear by either merging or being separated into different bundles. As a result, the van der Waals energy firstly decreases due to the aligning and bundling, and then rises up when being separated or further sliding between bundles. During the whole process the bending energy of carbon nanotubes is reduced.

It should be noticed that the aforementioned microstructural evolution mechanisms dissipate energy and require driven forces from external loads. The evolution occurs throughout the whole material during the tensile process and presents a hierarchical nature. Single carbon nanotubes form bundles, bridges by increased contact with other tubes and the bundles can form larger bundles and bridges with adjacent bundles. The whole process is thus very complicated and is expected to depend on many factors including temperature, loading rate, *etc*. The networked structure

will eventually evolve into the one shown in Fig. 3. Further loading will lead to local failure of intertube binding.

Discussion

Relation between microstructures and mechanical properties

With the mechanisms extracted above we can now map the microstructural evolution to the network's overall load-bearing and transfer capacities. The free energy of the system is $F = E - TS$ where T is the temperature and S is configurational entropy of the network, and the potential energy E_{tot} is

$$E_{tot} = E_{stretch} + E_{bend} + E_{vdW} \quad (1)$$

As indicated in Fig. 1, the network structure after equilibration is fully relaxed at local minima within the global energy landscape. When the tensile load is initially applied to the network, the load is mostly carried by the intertube interaction as the covalent bond is much stiffer than the van der Waals binding between carbon nanotubes. As a result, we observe a significant energy increase arising from E_{vdW}, as shown in Fig. 6(c). When the bundling process starts, the intertube cohesive energy E_{vdW} lowers. The intratube covalent bond bears more loads in the network. As shown in Fig. 6(b), the bundling and bending of bridging nanotubes lead to increasing of E_{bend}, while the alignment of bridging nanotubes results in reduction of the bending energy.

The force chains, or the nanotubes that are bearing most of the axial loads, are serial combinations of intratube load transfer elements through covalent bonds ($F_{streching}$ and $F_{bending}$) and intertube load transfer elements through van der Waals interaction (F_{pair}). As the former has a much higher tensile strength in comparison to the later one, $F_{streching}$ dominantly carries the load as shown in Fig. 6(a), while F_{pair} and F_{angle} have a lesser contribution. As an increasing axial load eventually exceeds the shear strength between the carbon nanotubes in the force chains, the network starts to fail at the intertube interface. As a result, the whole network eventually separates into several blocks. Within each block the network structure is well preserved, while between blocks is the pull-out failure of the carbon nanotube bundles.[6,20] As the relative sliding between neighbouring nanotubes leads to significant extension along the tensile direction, the tensile force–strain curve thus gradually decays with a long tail that indicates a high material toughness.

Moreover, the entropic part of the free energy $-TS$ increases along the tensile process due to both the bundling and aligning processes. So the elasticity shown in Fig. 2 is attributed to both entropic elasticity and elastic deformation. The structural evolution cannot be reversed because of locking at minima in the complicated energy landscape.

Failure mechanism and mechanical enhancement of carbon nanotube networks

The deformation and failure mechanism of carbon nanotubes networks is distinctly different from conventional brittle materials where structure breaks into part tensile when the stress reaches the intrinsic strength. The van der Waals interactions between carbon nanotubes define the deformation and microstructural evolution. The mechanical resistance to intertube sliding is extremely low in the carbon nanotubes with pristine carbon nanotubes, thus the network structure fails at the weakest region, *i.e.* at the intertube interfaces. As shown before, under elevated loads, the whole material is separated into several blocks with relatively smaller deformation within these blocks, which are interconnected through carbon nanotube bundles where pull-out failure occurs. Its strength thus is defined by the shear strength. The force borne by the material gradually decreases as the contact area and van der Waals cohesion energy is reduced. This failure mechanism is reminiscent of that of ductile materials such as metals, where tensile loads firstly nucleate dislocations that subsequently lead to plastic behaviour with a plateau or stiffening in the force–strain curve.

From these insights, we can enhance the mechanical properties of carbon nanotube networks by prohibiting the intertube sliding during the loading process and improving the deformation affinity.

Biaxial loading

With a close inspection of the structural evolving patterns in Fig. 3, it is noticeable that the deformation affinity and topology of network deformation can be much preserved if a multi-axial stress state is reached. We thus perform biaxial tension simulations on the same network structure as investigated in the uniaxial studies. As shown in Fig. 8 and 9(a)–(d) and Movie M2 in the Supporting Information,† the structural pattern is much more uniform and affine than that under uniaxial loading. In the y direction, covalent bonds, instead of van der Waals interactions as in the uniaxial loading condition, carry the loads. The contraction induced bending and aligning processes disappear here. The microstructural evolution is shown to be a combination of isotropic expansion and remarkably intertube bundling, which lead to the formation of a porous structure with increasing pore size and a failure mechanism by interfiber sliding within the backbones.

Cross-links

Another approach to enhance the mechanical properties of a network is to introduce cross-links between carbon nanotubes, as inspired by biological materials such as the cytoskeleton or collagen networks.[7,21] Chemical bonds mediated by polymers or

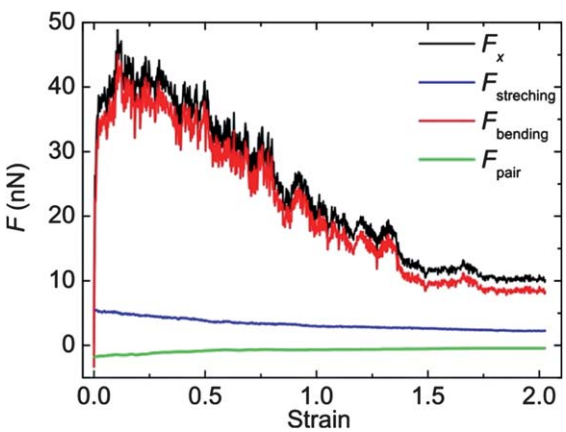

Fig. 8 Force sustained in the carbon nanotube networks biaxial tensile loading, as separated into stretching, bending and pair components.

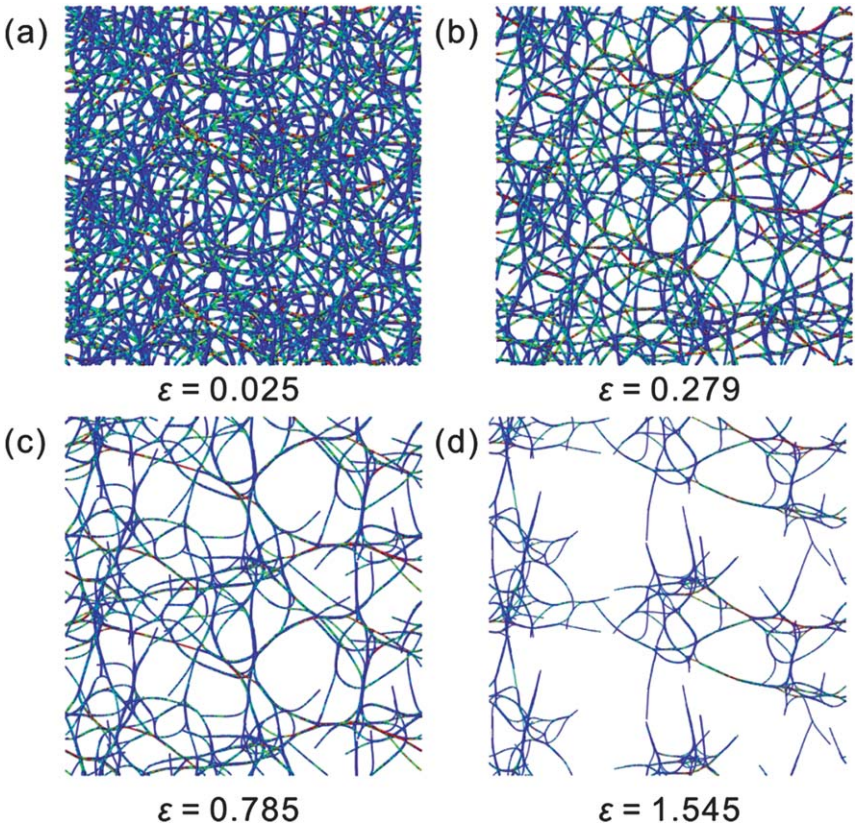

Fig. 9 Structural evolution of the carbon nanotube network with strain at (a) 0.025%, (b) 0.279, (c) 0.785, (d) 1.545. The color maps stress amplitude along the tensile direction. The blue color represents zero or compressive stress, while other colors indicate the tensile stress state and the red color corresponds with the maximum stress value. The network structure is duplicated in the *y* direction for better illustration.

molecules can significantly enhance the load transfer between carbon nanostructures. This is evidenced by a number of recent studies on buckypapers and graphene papers where coordinative bonds, polymer cross-links effectively improve their overall mechanical properties.[22–27]

To investigate the effects of cross-links on the mechanical properties of carbon nanotube networks, we introduce covalent cross-links that are 10% of the total intertube contacts. The cross-link has the same spring constant as the one used for intratube stretching terms but an equilibrium distance that includes the carbon nanotube diameters. We perform uniaxial loading simulations and the results are summarized in Fig. 10. We find that the network topology has negligible change during the tensile process. The stress distribution is uniform throughout the network in the tensile direction. As a result, as the load increases and it is dominantly borne by the elongation of covalent bonds in the carbon nanotubes.

It should be noticed that the length of the carbon nanotubes here is 100 nm, much shorter than its persistence length L_p in the range of 10–100 μm.[28] As their lengths exceed L_p, carbon nanotubes become curvy and entanglement between them will lead to more complexity to the mechanical behaviour of networks.

Organized network structures

In addition, to fabricate carbon nanotube networks with a regular lattice structure, while difficult to achieve, is a rational approach to design their mechanical properties. Experiments on the carbon nanotube sheets show that the mechanical properties, especially the Poisson's ratio, of the sheets can be well controlled by the structural and mechanical characteristics such as the nanotube orientation, force constants of bending and intertube torsion deformations. With a careful selection of these parameters, these designs can even provide materials with a negative Poisson's ratio. Although it is not observed for our network structures here (Fig. 6(d)), there are several reports that reveal a correlation between specific microstructures with a sign change of Poisson's ratio, with interesting applications including protecting clothing, automotive and aerospace industries.[7,29,30]

Metastable states and viscoelastic behaviour

As mentioned in previous discussion on structural evolution, the energy landscape of the carbon nanotube networks is complicated because of the co-existence of local bundling, bending and crossing structures. A simple presentation of this complexity is shown in Fig. 11. After applying uniaxial loads at specific levels, we maintain the strain of the whole network and track evolution of the total potential energy E. We find that E converges at those strain values, suggesting that microstructural evolution is driven by mechanical loads. This result also indicates metastable thermodynamic states trapped at local minima of the potential energy landscape. These metastable states directly reflect

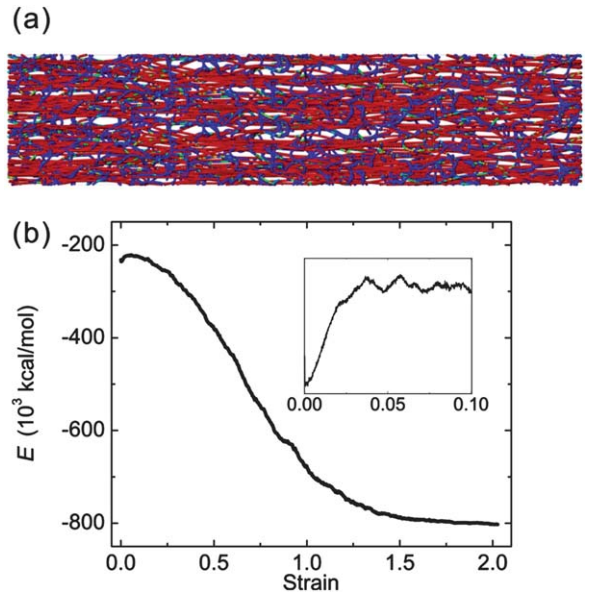

Fig. 10 Mechanical properties of carbon nanotube networks with covalent cross-links (10% of the contacts) introduced between adjacent carbon nanotubes. (a) Stress distribution in the cross-linked carbon nanotube network. The colour maps stress amplitude along the tensile direction. The blue colour represents zero or compressive stress, while other colours indicate the tensile stress state and the red colour corresponds to the maximum stress value. The network structure is duplicated in the *y* direction for better illustration. (b) Evolution of total energy *E* as a uniaxial strain load is applied.

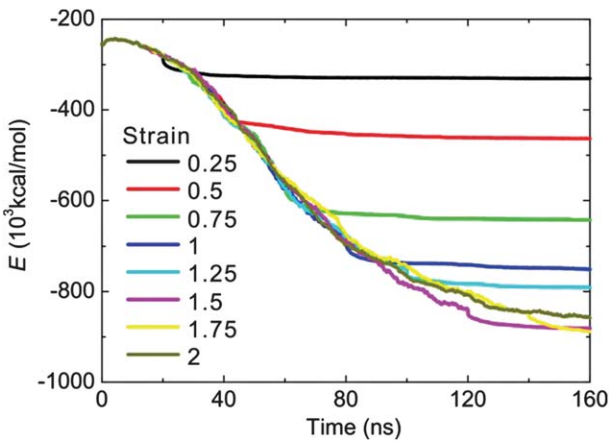

Fig. 11 Evolution of total potential energy *E* while the carbon nanotube network is experiencing constant uniaxial strain loads at different values as annotated.

viscoelastic properties of carbon nanotube networks that will be investigated in our future studies.[6,31]

Conclusions

In conclusion, we have performed coarse-grained molecular dynamics simulations for the mechanics of carbon nanotube networks. Microstructural characteristics and evolution of the networks under mechanical loads are analysed, and their correlation with macroscopic mechanical behaviour is discussed. Based on our simulation results and insights as obtained, strategies to enhance their mechanical performance are proposed, *e.g.* by improving the strain affinity in multi-axial loading conditions or introducing intertube cross-links to avoid pull-out failure that directly leads to localized failure of the material. The coarse-grained scheme utilized here can also be extended to other networked materials including carbon nanotube sponges, semi-flexible biopolymers and polymer microframes, which could help a comparative study of these disperse materials for a boarder view of new materials design.[32–34]

Acknowledgements

This work is supported by Tsinghua University through the Key Talent Support Program, and the National Science Foundation of China through Young Scholar Grant 11002079 (Z.X.). The molecular dynamics simulations are supported by Shanghai Supercomputer Center of China.

Notes and references

1 B. D. Gates, *Science*, 2009, **323**, 1566–1567.
2 H. Nishide and K. Oyaizu, *Science*, 2008, **319**, 737–738.
3 O. Hod, E. Rabani and R. Baer, *Phys. Rev. B*, 2003, **67**, 195408.
4 J. Z. Liu, Q. Zheng and Q. Jiang, *Phys. Rev. Lett.*, 2001, **86**, 4843–4847.
5 B. K. Satapathy, M. Ganß, P. Pötschke and R. Weidisch, *Stress Transfer and Fracture Mechanisms in Carbon Nanotube-Reinforced Polymer Nanocomposites*, Wiley-VCH Verlag GmbH & Co. KGaA, 2010.
6 M. Xu, D. N. Futaba, T. Yamada, M. Yumura and K. Hata, *Science*, 2010, **330**, 1364–1368.
7 L. J. Hall, V. R. Coluci, D. S. Galvão, M. E. Kozlov, M. Zhang, S. O. Dantas and R. H. Baughman, *Science*, 2008, **320**, 504–507.
8 B. Vigolo, A. Pénicaud, C. Coulon, C. Sauder, R. Pailler, C. Journet, P. Bernier and P. Poulin, *Science*, 2000, **290**, 1331–1334.
9 S. M. Cooper, H. F. Chuang, M. Cinke, B. A. Cruden and M. Meyyappan, *Nano Lett.*, 2003, **3**, 189–192.
10 R. C. Picu, *Soft Matter*, 2011, **7**, 6768–6785.
11 F. Deng, M. Ito, T. Noguchi, L. Wang, H. Ueki, K.-i. Niihara, Y. A. Kim, M. Endo and Q.-S. Zheng, *ACS Nano*, 2011, **5**, 3858–3866.
12 K. E. Kasza, A. C. Rowat, J. Liu, T. E. Angelini, C. P. Brangwynne, G. H. Koenderink and D. A. Weitz, *Curr. Opin. Cell Biol.*, 2007, **19**, 101–107.
13 A. N. Volkov and L. V. Zhigilei, *ACS Nano*, 2010, **4**, 6187–6195.
14 S. W. Cranford and M. J. Buehler, *Nanotechnology*, 2010, **21**, 265706–265712.
15 L. Deng, X. Trepat, J. P. Butler, E. Millet, K. G. Morgan, D. A. Weitz and J. J. Fredberg, *Nat. Mater.*, 2006, **5**, 636–640.
16 B. Ashrafi, J. Guan, V. Mirjalili, P. Hubert, B. Simard and A. Johnston, *Composites, Part A*, 2010, **41**, 1184–1191.
17 R. L. D. Whitby, T. Fukuda, T. Maekawa, S. L. James and S. V. Mikhalovsky, *Carbon*, 2008, **46**, 949–956.
18 S. Cranford, H. Yao, C. Ortiz and M. J. Buehler, *J. Mech. Phys. Solids*, 2010, **58**, 409–427.
19 D. Qian, W. K. Liu and R. S. Ruoff, *Compos. Sci. Technol.*, 2003, **63**, 1561–1569.
20 D. Qian, E. C. Dickey, R. Andrews and T. Rantell, *Appl. Phys. Lett.*, 2000, **76**, 2868–2870.
21 M. J. Buehler, *Proc. Natl. Acad. Sci. U. S. A.*, 2006, **103**, 12285–12290.
22 Y. Liu, B. Xie and Z. Xu, *J. Mater. Chem.*, 2011, **21**, 6707–6712.
23 B. Peng, M. Locascio, P. Zapol, S. Li, S. L. Mielke, G. C. Schatz and H. D. Espinosa, *Nat. Nanotechnol.*, 2008, **3**, 626–631.
24 Y. C. Zhang, A. A. Broekhuis, M. C. A. Stuart, T. F. Landaluce, D. Fausti, P. Rudolf and F. Picchioni, *Macromolecules*, 2008, **41**, 6141–6146.
25 G. H. Bratzel, S. W. Cranford, H. Espinosa and M. J. Buehler, *J. Mater. Chem.*, 2010, **20**, 10465–10474.
26 A. Satti, A. Perret, J. E. McCarthy and Y. K. Gun'ko, *J. Mater. Chem.*, 2010, **20**, 7941–7943.

27 H. Cheng, G. P. Pez and A. C. Cooper, *Nano Lett.*, 2003, **3**, 585–587.
28 N. Fakhri, D. A. Tsyboulski, L. Cognet, R. B. Weisman and M. Pasquali, *Proc. Natl. Acad. Sci. U. S. A.*, 2009, **106**, 14219–14223.
29 V. R. Coluci, L. J. Hall, M. E. Kozlov, M. Zhang, S. O. Dantas, D. S. o. Galv atilde and R. H. Baughman, *Phys. Rev. B: Condens. Matter Mater. Phys.*, 2008, **78**, 115408.
30 Y. J. Ma, X. F. Yao, Q. S. Zheng, Y. Yin, D. Jiang, G. H. Xu, F. Wei and Q. Zhang, *Appl. Phys. Lett.*, 2010, **97**, 061909–3.
31 S. V. Ahir, E. M. Terentjev, S. X. Lu and B. Panchapakesan, *Phys. Rev. B: Condens. Matter Mater. Phys.*, 2007, **76**, 165437.
32 J.-H. Lee, L. Wang, S. Kooi, M. C. Boyce and E. L. Thomas, *Nano Lett.*, 2010, **10**, 2592–2597.
33 L. Wang, M. C. Boyce, C.-Y. Wen and E. L. Thomas, *Adv. Funct. Mater.*, 2009, **19**, 1343–1350.
34 H. Li, X. Gui, L. Zhang, C. Ji, Y. Zhang, P. Sun, J. Wei, K. Wang, H. Zhu, D. Wu and A. Cao, *Adv. Funct. Mater.*, 2011, DOI: 10.1002/adfm.201100823.